Real-time spectral interleaved electro-optic dual-comb spectroscopy

BINGXIN XU,[1] XINYUFAN,[1,*] SHUAI WANG, [1] AND ZUYUAN HE[1,2]

[1] *State Key Laboratory of Advanced Optical Communication Systems and Networks, Department of Electronic Engineering, Shanghai Jiao Tong University, Shanghai 200240, China*

[2] *zuyuanhe@sjtu.edu.cn*

[*] *fan.xinyu@sjtu.edu.cn*

Abstract: Optical frequency comb with evenly spaced lines over a broad bandwidth has revolutionized the fields of optical metrology and spectroscopy. Here, we propose an electro-optic dual-comb spectroscopy to real-time interleave the spectrum with high resolution, in which two electro-optic frequency combs are seed by swept light source. An interleaved spectrum with a high resolution is real-time recorded by the sweeping probe comb without gap time, which is multi-heterodyne detected by the sweeping local comb. The proposed scheme measures a spectrum spanning 304 GHz in 1.6 ms with a resolution of 1 MHz, and reaches a spectral sampling rate of 1.9×10^8 points/s under Nyquist-limitation. A reflectance spectrum is measured with a calculated figure-of-merit of 4.2×10^8, which shows great prospect for fast and high-resolution applications.

1. Introduction

Optical frequency combs (OFCs) [1, 2], originally built from femtosecond mode-locked lasers, have revolutionized the field of spectroscopy with phase coherent spectral lines and broad bandwidth [3–5]. Several techniques are developed to extract the spectroscopic content encoded on the comb light, such as virtually imaged phased arrays (VIPA)-based spectroscopy [6] and Fourier transform spectroscopy (FTS) [7]. Dual-comb spectroscopy (DCS) emerges from comb-based techniques and has been implemented in linear spectroscopy [8–13], nonlinear spectroscopy [14, 15] and microscopy [16, 17]. Beating two OFCs with slightly different repetition rates, DCS retrieves each frequency component in radio frequency (RF) domain, which may fully exploit the spectral resolution and measurement bandwidth determined by OFCs. The spectral resolution can be further reduced to kHz less than line-spacing by time-consuming spectral interleave techniques [13, 18, 19]. In recent years, novel approaches for OFC generation have been explored, which facilitate DCS performed at different wavebands with versatility [9, 11, 12].

Mutual coherence establishment between two independent combs requires phase-locking circuits [10, 20] or phase correction [21–23]. OFCs may also be generated by electro-optic modulation from a single seed laser to form a DCS system with intrinsic mutual coherence [24–31], which significantly reduces the system complexity. Electro-optic frequency combs (EOFCs) [32, 33] have been demonstrated with nonlinearly broadened bandwidth [34] or ultra-dense line-spacing [35, 36], which promotes flexible electro-optic DCS for various spectroscopic applications.

Laser swept spectroscopy (LSS) is another widely used method to obtain the optical spectrum point by point by sweeping the wavelength in different ways [37, 38]. Internally swept laser may scan a wide spectrum over 100 nm range with poor nonlinearity. Relatively, external modulation [39–41] using the chirped electrical signal is an effective way to realize the theoretical sub-MHz resolution with tens of GHz frequency range limited by modulators and RF generators.

In this paper, we propose a novel DCS technique with real-time interleaved spectrum, which simultaneously have high spectral resolution, large bandwidth and fast measurement speed. A

Research Square

Preprints are preliminary reports that have not undergone peer review. They should not be considered conclusive, used to inform clinical practice, or referenced by the media as validated information.

linearly swept light source serves as the seed of two EOFCs, which have a slight repetition rate difference to build a dual-comb interferometer. Each comb-line pair records a spectrum with a high resolution and a limited range. The sweep range is in accordance with the repetition rate of the probe comb to realize the full coverage of total bandwidth with simultaneous sweeping of all comb teeth. The dual-comb interferometer locates each comb-line pair to different frequencies in electrical domain. So the spectrum information loaded on each comb tooth can be separated by using a digital filter, and the total spectrum can be recovered from all the EOFC teeth. In the experiment, a spectrum covering 304 GHz bandwidth with 1 MHz spectral resolution is recorded. Considering the measurement time of 1.6 ms, the demonstration shows a sampling-rate of 1.9 $\times 10^8$ points/s. Besides, the proposed method realizes 4.2×10^8 figure-of-merit thanks to the capability of simultaneously recording all channels without gap time.

2. Operation Principle

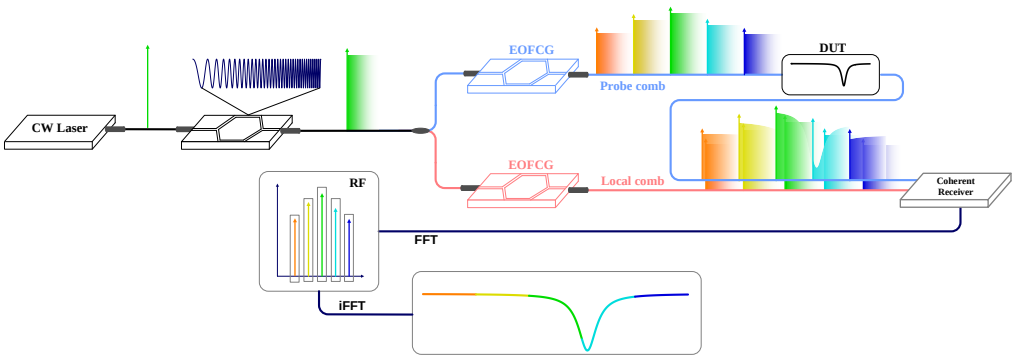

Fig. 1. The schematic to show the operation principle of proposed EO-DCS with real-time interleaved spectrum. CW laser: continuous-wave laser; EOFCG: electro-optic frequency comb generation; DUT: Device-under-test; RF: radio frequency; FFT: fast Fourier transformation; iFFT: inverse fast Fourier transformation.

The operation principle is illustrated in Fig. 1. This method consists of two primary components, which are respectively an ultra-linearly frequency-swept optical source generation system and an electro-optic dual-comb interferometer system. A frequency stabilized laser seeds the swept optical source by using external modulation, which utilizes the ultra-high linearity of the electrical sweeping signal to realize the sweep of the optical frequency. The optical source with a sweep range of B_s and a nonlinear error of $\delta\mu$ feeds the followed-up electro-optic dual-comb interferometer, in which two EOFCs with line-spacing of f_p and f_l are generated. The probe comb passes the device under test (DUT) to record its absorption spectrum property. Since the probe comb is sweeping, each comb line measures a bandwidth of B_s instead of a single point in conventional DCS system, and the measurement results may be spliced when $f_p \leq B_s$. The local comb is simultaneously swept to locate each probe comb line to separated frequencies in RF domain with an interval of $\Delta f = f_p - f_l$. Therefore, the recorded spectrum of each channel can be retrieved by using a digital filter to distinguish.

3. Experimental setup and results

A specific experimental setup of the DCS system is depicted in Fig. 2. A continuous-wave fiber laser (NKT, Adjustik E15) is locked to a stable cavity with finesse of 400 k and daily drift of less than 100 kHz by using Pound-Drever-Hall technique. The output of the stabilized laser is modulated by a Mach-Zehnder modulator (MZM), which is driven by an arbitrary waveform

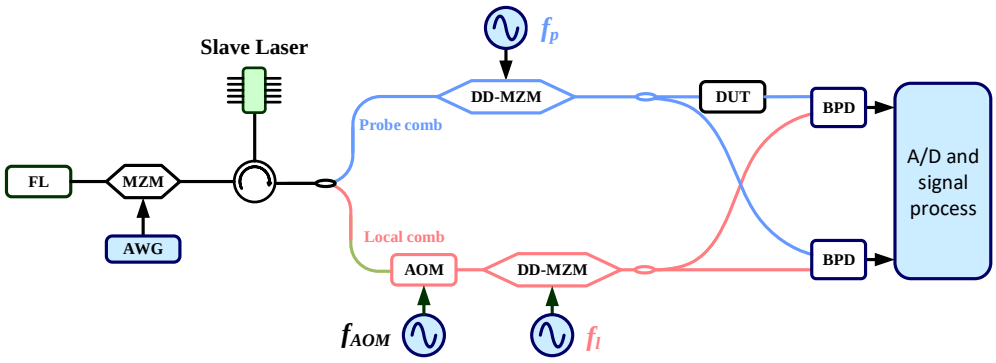

Fig. 2. Experimental setup of the proposed EO-DCS system. FL: fiber laser; MZM: Mach-Zehnder modulator; AWG: arbitrary waveform generator; AOM: acousto-optic modulator; DD-MZM: dual-drive Mach-Zehnder modulator; DUT: Device-under-test; BPD: balanced photo-detector.

generator (AWG, Keysight M8195A) with a sampling rate of 64 GS/s. The electrically driven RF signal is a sinusoidal signal with a frequency linearly swept from 2 GHz to 18 GHz in 1.6 ms. The linearly-swept sideband is generated after the modulation, and then injected into an isolator-removed distributed feedback laser diode (DFB-LD) which serves as a slave laser via an optical circulator. Due to the injection locking effect, the 1st-order positive sideband is selected and amplified to 10 mW, and the carrier and all other sidebands are suppressed with an extinction ratio of over 20 dB. Therefore, a linearly-swept lightwave with low power fluctuation is generated. We characterize the property of the swept lightwave by using an unbalanced Mach-Zehnder interferometer with 1 km delay fiber. As shown in Fig. 3(a), this lightwave sweeps 16 GHz bandwidth in 1.6 ms with a nonlinear error of 9.13 kHz standard deviation.

Then, the swept lightwave is used as the light source of the electro-optic dual-comb interferometer. Two dual-drive MZMs (DD-MZMs) with low half-wave voltage (2.5 V@25 GHz) are used to generate the probe and local EOFCs with line spacing of f_p=16 GHz and f_l=15.99 GHz with a detune Δf of 10 MHz. The electrical signals generated by RF microwave sources are separated in parallel to be amplified to 3 Watts each to drive the modulators. Then the high-order sidebands are generated and flattened by adjusting the phase shift and the current bias to satisfy the flat spectrum conditions [32]. An acousto-optic modulator (AOM) introduces a frequency shift f_{AOM}=200 MHz in the local branch to avoid the overlapping between the positive and negative sidebands. The optical spectra of the probe comb and local comb are shown in Fig. 3(b) and 3(c), which are measured by using an optical spectrometer with a resolution of 2 GHz. The optical spectrum of the probe comb, when the seed lightwave is sweeping, is also shown in Fig. 3(b). The probe EOFC passes through a device under test (DUT) and then interferes with the local EOFC. A reference branch without samples is introduced to compensate the power unevenness of each comb line and the power fluctuation during the frequency sweeping. The interference signals are detected by a balanced photo-detector (BPD, Thorlabs PDB470C) with a bandwidth of 400 MHz to be an electrical RF comb with a line-spacing of Δf, and digitized by a digital oscilloscope (Keysight DSOS204A) with a sampling rate of 1 GS/s.

A temporal data of reference branch recorded in 1.6 ms is shown in Fig. 4(a), which has a stable power thanks to the optical injection locking. A zoom-in figure containing four interferograms in 0.4 μs is shown in Fig. 4(b), and the non-pulse waveform may reduce the quantization noise. As depicted in Fig. 4(c), the electrical spectrum is obtained by digital Fourier transformation, which contains flat 19 lines with averaged power of -19.27 dBm. The center frequency is located at 200 MHz with a small detune introduced by the optical path difference. Each channel is equally

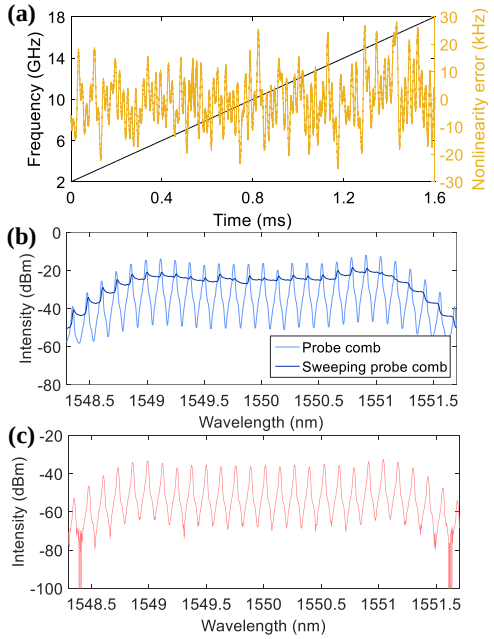

Fig. 3. (a) Sweep range and nonlinear error of the ultra-linearly swept optical source measured by using an unbalanced Mach-Zehnder interferometer; (b) Optical spectrum of the probe comb with a stabilized optical source and a linearly-swept optical source; (c) Optical spectrum of the local comb with a stabilized optical source.

spaced with an interval of Δf=10 MHz to be distinguished in frequency domain.

A reflectance spectrum of a fiber Fabry-Perot interferometer (FFPI) is measured by using the proposed system. The FFPI is composed of a pair of high reflection fiber Bragg grating (FBG) with reflectivity of 99 %. The electrical spectrum of the reflected probe comb is also shown in Fig. 4(c). A digital filter is used to select the 3-rd channel for demodulation, and the zoom-in electrical spectrum is shown in Fig. 4(d). The temporal waveform of the 3-rd channel is a sinusoidal signal, whose varying intensity in 1.6 ms represents the optical spectrum of the FFPI in a bandwidth of 16 GHz. The envelope extracted by a digital Hilbert transformation is moving averaged with 100 points window, and reaches a temporal resolution of 100 ns corresponding to the demodulation filter bandwidth of 10 MHz. The waveform and the envelope are shown in Fig. 4(e), and a zoom-in figure with a duration of 1 μs is shown in Fig. 4(f). The adjacent points of envelope have a frequency change of 1 MHz during the sweeping. The actual reflectance spectrum is obtained by a calibration process compared with the reference branch without samples to compensate the power variation. The calibrated spectrum spanning 304 GHz bandwidth is shown in Fig. 5(a), which is obtained by successive demodulation of the total 19 lines. The frequency accuracy of the splicing process is ensured since all RF generators are synchronous to a same oscillator. As shown in Fig. 5(b), the spectrum of the deepest resonance centered at a relative frequency of 61.45 GHz is demodulated with a half maximum (FWHM) of about 5 MHz. The linear residual error spanning 2 GHz bandwidth without measured spectrum is used to calculated the measurement signal-to-noise ratio (SNR), as shown in Fig. 5(c). The standard deviation is 0.0151, corresponding to a SNR of 66.23. Since the power difference between the demodulation channel and the averaged power is 0.78 dBm, the averaged SNR of all results is calculated to be 55.34. The figure of merit ($SNR_f * M/\sqrt{\tau}$, SNR_f is the averaged SNR, M is the demodulation points, and τ is the measurement time) is calculated to be 4.2×10^8. The total spectrum spanning

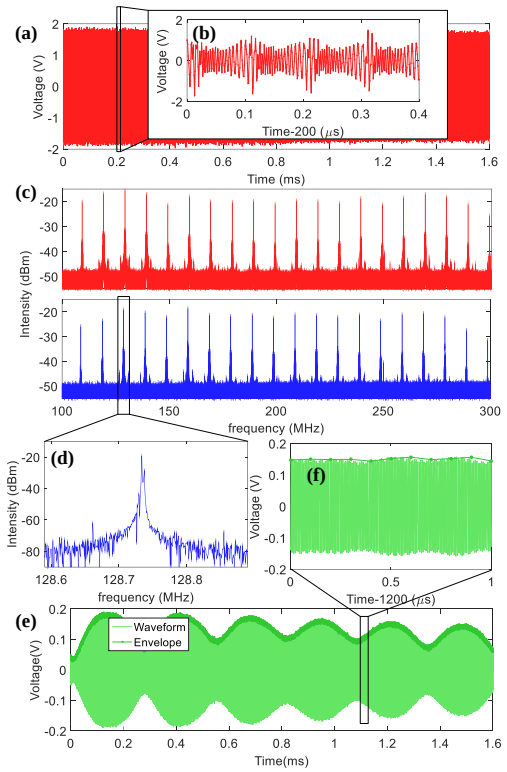

Fig. 4. (a) Temporal waveform of dual-comb interferometer recorded in 1.6 ms with a sampling rate of 1 GS/s; (b) zoom-in figure of (a) in 0.4 μs; (c) Electrical spectrum of the probe comb reflected by the FFPI containing total 19 lines centered at about 200 MHz; (d) Zoom-in figure of the 3-rd channel to be filtered for the demodulation; (e) Temporal waveform and envelope of the 3-rd channel obtained by digital inverse Fourier transformation; (f) Zoom-in figure of (e) with a time length of 50 ns starting from 0.4 ms.

304 GHz with a resolution of 1 MHz is recorded in 1.6 ms, corresponding to an equivalent spectral sampling rate of 1.9×10^8 Sample/s, which almost reaches Nyquist-limitation thanks to the real-time interleaving.

4. Conclusions

In conclusion, we propose a novel DCS technique with ultra-high spectral acquisition rate implemented by EOFCs seeded by a linearly frequency-swept light source. This method retrieves a spectrum in 1.6 ms with a spectral resolution of 1 MHz and a bandwidth of 304 GHz. With real-time interleaved spectrum, the proposed method realizes a spectral sampling-rate of 1.9×10^8 points/s under Nyquist-limitation. The spectroscopic results of a FFPI reflectance spectrum validate the novel method, and the averaged SNR reaches 55.34 in 1.6 ms measurement time, corresponding to a figure of merit of 4.2×10^8. This paper provides an effective method based on EOFCs for fast high-spectral-resolution measurement applications such as measuring high-Q cavity, electro-magnetically induced transparency, or physical and biochemical sensing requiring hyperfine spectrum measurement.

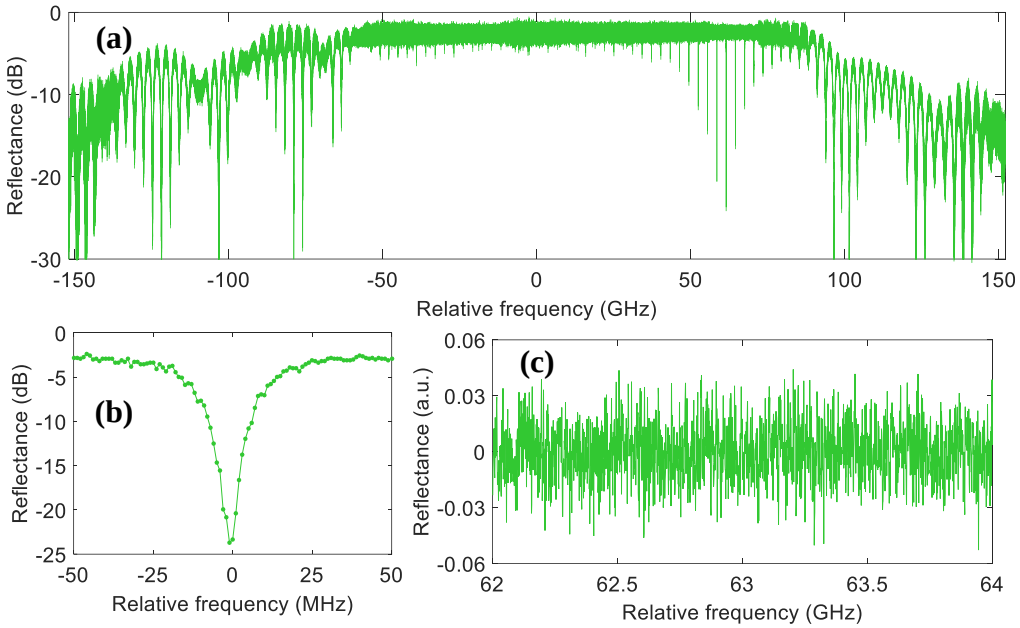

Fig. 5. (a) Reflectance of the FFPI spanning 304 GHz bandwidth with a resolution of 1 MHz recorded in 1.6 ms, which is demodulated and spliced from total 19 channels; (b) A zoom-in result of the deepest resonance peak with a FWHM of 5 MHz ; (c) Linear residual error spanning 2 GHz bandwidth without measured spectrum with a standard deviation of 0.0151.

Funding

National Key R&D Program of China under Grant 2017YFB0405500 and National Natural Science Foundation of China (NSFC) under Grant 61775132, 61735015, 61620106015.

Disclosures

The authors declare no conflicts of interest.

References

1. T. W. Hänsch, "Nobel lecture: Passion for precision," Rev. Mod. Phys. **78**, 1297–1309 (2006).
2. S. A. Diddams, "The evolving optical frequency comb," J. Opt. Soc. Am. B **27**, B51–B62 (2010).
3. D. J. Jones, S. A. Diddams, J. K. Ranka, A. Stentz, R. S. Windeler, J. L. Hall, and S. T. Cundiff, "Carrier-envelope phase control of femtosecond mode-locked lasers and direct optical frequency synthesis," Science **288**, 635–639 (2000).
4. N. R. Newbury, "Searching for applications with a fine-tooth comb," Nat. Photonics **5**, 186–188 (2011).
5. N. Picqué and T. W. Hänsch, "Frequency comb spectroscopy," Nat. Photonics **13**, 146–157 (2019).
6. S. A. Diddams, L. Hollberg, and V. Mbele, "Molecular fingerprinting with the resolved modes of a femtosecond laser frequency comb," Nature **445**, 627–630 (2007).
7. J. Mandon, G. Guelachvili, and N. Picqué, "Fourier transform spectroscopy with a laser frequency comb," Nat. Photonics **3**, 99–102 (2009).
8. G. Ycas, F. R. Giorgetta, E. Baumann, I. Coddington, D. Herman, S. A. Diddams, and N. R. Newbury, "High-coherence mid-infrared dual-comb spectroscopy spanning 2.6 to 5.2m," Nat. Photonics **12**, 202–208 (2018).
9. M. Rosch, G. Scalari, G. Villares, L. Bosco, M. Beck, and J. Faist, "On-chip, self-detected terahertz dual-comb source," Appl. Phys. Lett. **108**, 171104 (2016).
10. I. Coddington, W. C. Swann, and N. R. Newbury, "Coherent multiheterodyne spectroscopy using stabilized optical frequency combs," Phys. Rev. Lett. **100**, 013902 (2008).
11. S. M. Link, D. J. Maas, D. Waldburger, and U. Keller, "Dual-comb spectroscopy of water vapor with a free-running semiconductor disk laser," Science **356**, 1164–1168 (2017).

12. A. Hugi, G. Villares, S. Blaser, H. Liu, and J. Faist, "Mid-infrared frequency comb based on a quantum cascade laser," Nature **492**, 229 (2012).
13. S. A. Meek, A. Hipke, G. Guelachvili, T. W. Hänsch, and N. Picqué, "Doppler-free fourier transform spectroscopy," Opt. Lett. **43**, 162–165 (2018).
14. T. Ideguchi, B. Bernhardt, G. Guelachvili, T. W. Hänsch, and N. Picqué, "Raman-induced kerr-effect dual-comb spectroscopy," Opt. Lett. **37**, 4498–4500 (2012).
15. T. Ideguchi, S. Holzner, B. Bernhardt, G. Guelachvili, N. Picqué, and T. W. Hänsch, "Coherent raman spectro-imaging with laser frequency combs," Nature **502**, 355 (2013).
16. E. Hase, T. Minamikawa, T. Mizuno, S. Miyamoto, R. Ichikawa, Y.-D. Hsieh, K. Shibuya, K. Sato, Y. Nakajima, A. Asahara, K. Minoshima, Y. Mizutani, T. Iwata, H. Yamamoto, and T. Yasui, "Scan-less confocal phase imaging based on dual-comb microscopy," Optica **5**, 634–643 (2018).
17. P. Feng, J. Kang, S. Tan, Y.-X. Ren, C. Zhang, and K. K. Y. Wong, "Dual-comb spectrally encoded confocal microscopy by electro-optic modulators," Opt. Lett. **44**, 2919–2922 (2019).
18. P. Jacquet, J. Mandon, B. Bernhardt, R. Holzwarth, G. Guelachvili, T. W. Hänsch, and N. Picqué, "Frequency comb fourier transform spectroscopy with khz optical resolution," in *Advances in Imaging,* (Optical Society of America, 2009), p. FMB2.
19. E. Baumann, F. R. Giorgetta, W. C. Swann, A. M. Zolot, I. Coddington, and N. R. Newbury, "Spectroscopy of the methane ν_3 band with an accurate midinfrared coherent dual-comb spectrometer," Phys. Rev. A **84**, 062513 (2011).
20. A. M. Zolot, F. R. Giorgetta, E. Baumann, J. W. Nicholson, W. C. Swann, I. Coddington, and N. R. Newbury, "Direct-comb molecular spectroscopy with accurate, resolved comb teeth over 43 thz," Opt. Lett. **37**, 638–640 (2012).
21. T. Ideguchi, A. Poisson, G. Guelachvili, N. Picqué, and T. W. H$\acute{}$ansch, "Adaptive real-time dual-comb spectroscopy," Nat. Commun. **5**, 3375 (2014).
22. J. Roy, J.-D. Deschênes, S. Potvin, and J. Genest, "Continuous real-time correction and averaging for frequency comb interferometry," Opt. Express **20**, 21932–21939 (2012).
23. Z. Chen, M. Yan, T. W. H$\acute{}$ansch, and N. Picqué, "A phase-stable dual-comb interferometer," Nat. Commun. **9**, 3035 (2018).
24. D. A. Long, A. J. Fleisher, K. O. Douglass, S. E. Maxwell, K. Bielska, J. T. Hodges, and D. F. Plusquellic, "Multiheterodyne spectroscopy with optical frequency combs generated from a continuous-wave laser," Opt. Lett. **39**, 2688–2690 (2014).
25. P. Martín-Mateos, B. Jerez, and P. Acedo, "Dual electro-optic optical frequency combs for multiheterodyne molecular dispersion spectroscopy," Opt. Express **23**, 21149–21158 (2015).
26. G. Millot, S. Pitois, M. Yan, T. Hovhannisyan, A. Bendahmane, T. W. Hänsch, and N. Picqué, "Frequency-agile dual-comb spectroscopy," Nat. Photonics **10**, 27 (2016).
27. V. Durán, P. A. Andrekson, and V. Torres-Company, "Electro-optic dual-comb interferometry over 40 nm bandwidth," Opt. Lett. **41**, 4190–4193 (2016).
28. M. Yan, P.-L. Luo, K. Iwakuni, G. Millot, T. W. Hänsch, and N. Picqué, "Mid-infrared dual-comb spectroscopy with electro-optic modulators," Light. Sci. & Appl. **6**, e17076 (2017).
29. K. Fdil, V. Michaud-Belleau, N. B. Hébert, P. Guay, A. J. Fleisher, J.-D. Deschênes, and J. Genest, "Dual electro-optic frequency comb spectroscopy using pseudo-random modulation," Opt. Lett. **44**, 4415–4418 (2019).
30. S. Wang, X. Fan, B. Xu, and Z. He, "Fast mhz spectral-resolution dual-comb spectroscopy with electro-optic modulators," Opt. Lett. **44**, 65–68 (2019).
31. B. Xu, X. Fan, S. Wang, and Z. He, "Broadband and high-resolution electro-optic dual-comb interferometer with frequency agility," Opt. Express **27**, 9266–9275 (2019).
32. T. Sakamoto, T. Kawanishi, and M. Izutsu, "Asymptotic formalism for ultraflat optical frequency comb generation using a mach-zehnder modulator," Opt. Lett. **32**, 1515–1517 (2007).
33. R. Wu, V. R. Supradeepa, C. M. Long, D. E. Leaird, and A. M. Weiner, "Generation of very flat optical frequency combs from continuous-wave lasers using cascaded intensity and phase modulators driven by tailored radio frequency waveforms," Opt. Lett. **35**, 3234–3236 (2010).
34. K. Beha, D. C. Cole, P. Del'Haye, A. Coillet, S. A. Diddams, and S. B. Papp, "Electronic synthesis of light," Optica **4**, 406–411 (2017).
35. Y. Bao, X. Yi, Z. Li, Q. Chen, J. Li, X. Fan, and X. Zhang, "A digitally generated ultrafine optical frequency comb for spectral measurements with 0.01-pm resolution and 0.7-μs response time," Light. Sci. & Appl. **4**, e300 (2015).
36. D. A. Long and B. J. Reschovsky, "Electro-optic frequency combs generated via direct digital synthesis applied to sub-doppler spectroscopy," OSA Continuum **2**, 3576–3583 (2019).
37. J. Zhu, S. K. Ozdemir, Y.-F. Xiao, L. Li, L. He, D.-R. Chen, and L. Yang, "On-chip single nanoparticle detection and sizing by mode splitting in an ultrahigh-q microresonator," Nat. Photonics **4**, 46–49 (2010).
38. P. Del'Haye, O. Arcizet, M. L. Gorodetsky, R. Holzwarth, and T. J. Kippenberg, "Frequency comb assisted diode laser spectroscopy for measurement of microcavity dispersion," Nat. Photonics **4**, 46–49 (2010).
39. F. Wei, B. Lu, J. Wang, D. Xu, Z. Pan, D. Chen, H. Cai, and R. Qu, "Precision and broadband frequency swept laser source based on high-order modulation-sideband injection-locking," Opt. Express **23**, 4970–4980 (2015).
40. S. Pan and M. Xue, "Ultrahigh-resolution optical vector analysis based on optical single-sideband modulation," J. Light. Technol. **35**, 836–845 (2017).
41. T. Qing, S. Li, Z. Tang, B. Gao, and S. Pan, "Optical vector analysis with attometer resolution, 90-db dynamic range

and thz bandwidth," Nat. Commun. **10**, 5135 (2019).